Pore Pressure Development in Liquefiable Soils Under Bi-Directional Loading Conditions

A. M. Kammerer[1], R.B. Seed [3], J. Wu[2], M. F. Riemer [3], and J. M. Pestana[3]
[1]Arup, San Francisco, California
[2]URS Corporation, Oakland, California
[3]Department of Civil and Environmental Engineering, University of California, Berkeley

Abstract—**A comprehensive testing database composed of modeling-quality, bi-directional cyclic simple shear testing on medium to high relative density, fully-saturated samples of Monterey 0/30 sand has recently been developed. This testing incorporated a variety of never before examined bi-directional stress paths on both level and sloping ground.**

Results from these tests have proven useful for enhancing current understanding of liquefaction behavior by allowing for a more complete theory to emerge. This new multi-dimensional theory greatly expands current understanding of liquefaction behavior and elucidates some areas in which current theory—which has been based principally on uni-directional testing—can be misleading or unconservative. Of particular interest are the topics of (a) pore pressure generation as a function of loading magnitude and direction, (b) the effects of sloping ground conditions, and (c) the post-liquefaction pore pressure behavior within each cycle.

This paper also describes the impact of bi-directional loading on maximum achievable pore pressures and reexamines the classic pore-pressure based definition of liquefaction as r_u =1.0 in light of recent results.

Keywords— **constitutive modeling, laboratory testing, liquefaction, multidirectional, sand, shear strain**

INTRODUCTION

Currently, the use of three-dimensional constitutive soil models in liquefaction problems is being hampered by a lack of high-quality, multi-directional laboratory test data for use in model development and calibration. To address this need, a program of simple shear testing was recently performed on medium to high relative density, fully-saturated sand samples under a variety of previously unexplored bi-directional stress paths. These stress paths incorporated three general categories: linear, oval/circular, and figure-8, as shown schematically in Fig 1. Tests were performed both with and without an initial static driving shear stress in order to replicate in-situ loading conditions on soils elements under both sloping and level ground conditions. Additionally, the major axis of the three loading types was oriented in both the dip and strike directions for the sloping ground cases.

The goals of this testing series are twofold. The first is the development of a high quality laboratory test database describing the behavior of liquefiable soils for use in model development and calibration. The second is the development of insight into the behavior of liquefiable soils under generalized loading conditions. The attainment of both of these goals required specialized sample preparation and testing techniques to be developed such that both the soil fabric and the imposed loading replicated the in-situ conditions to the extent possible.

LABORATORY TECHNIQUES, EQUIPMENT & MATERIAL

Testing was performed in the U.C. Berkeley Bi-directional Simple Shear Device [1], which is capable of applying cyclic horizontal shear stresses in two orthogonal directions, as well as cell and back pressures. For this testing series, 100mm (4-inch) diameter, 20mm (¾-inch) high, circular, clean sand samples were constructed using wet-pluviation. The samples were back-pressures saturated until B-values of 0.95 were reached to assure full saturation during testing. The samples were contained in NGI-style wire-reinforced latex membranes, which assured that K_o conditions were maintained.

Load control was used for both the horizontal shear stress and vertical normal stress. This was possible because undrained testing was performed on fully-saturated samples that were laterally confined by wire-reinforced membranes. This method allows for a direct measure of pore pressure to be recorded during testing.

Testing was performed on Monterey #0/30 sand, a highly uniform, medium sized, sub-rounded beach sand that was further prepared by the washing of the material over a #200 sieve to remove fine material. The D_{50} for the material is 0.36mm, the coefficient of uniformity (C_u) is

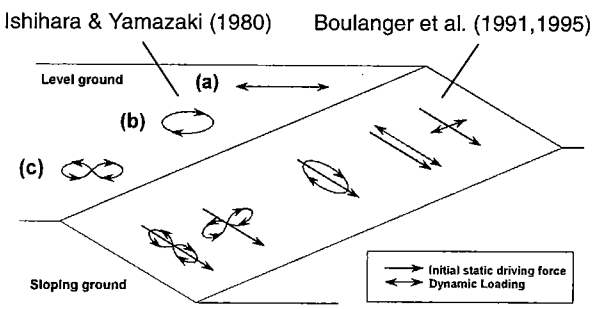

Fig. 1: Schematic illustration of idealized multi-directional loading

1.29, and the coefficient of curvature (C_c), is 0.98. A minimum void ratio of 0.541 was determined by the modified Japanese method and a maximum void ratio of 0.885 was determined by the dry tipping method.

Additional information on the laboratory program and material is provided in [2] and [3].

OVERVIEW OF TESTING PROGRAM

The database of tests developed consists of two complementary series. A comprehensive uni-directional test series by [3] was performed simultaneously and in conjunction with the bi-directional testing series described here in order to develop a well-verified basis from which to assess the influence of a load in a second horizontal direction. This testing incorporated four relative densities (30, 45, 60 and 80%) and three initial vertical effective stresses (40, 80 and 1.5 kPa).

The bi-directional series performed is summarized in Table 1. The schematics in the left column of the table represent the stress path categories shown schematically in Fig 1. The four additional columns separate the tests into "bins" based on stress level and density. Several parameters are shown for each test. These include the relative density (D_r), cyclic stress ratio in the principal direction (CSR_{max}), and the normalized initial static shear stress (α-value). The initial vertical effective stress (σ'_c) was 80kPa for all tests in the bi-directional series.

To assist those using the database for research purposes, a data quality classification (DQC) is also noted. The "A" classification denotes data of highest reliability. The "B" classification denotes data that is deemed less reliable. The reasons for the lower designation for each test is provided in [2]. In addition, some tests are also noted in multiple load path categories. Each test is first noted with the relevant information in the most appropriate category. Tests that are of interest in additional load path categories are then also noted in an italic font in the appropriate secondary category.

PARAMETER AND TESTING DEFINITIONS

Numerous terms and parameters have traditionally been used to describe both the state of a sample and the loading applied. However, some parameters require further specification to remove ambiguity arising from the multi-directional loading. Other parameters must be newly developed altogether. Several common terms have been made more precise by the addition of subscripts that include the terms "dip", "strike", "X", "Y", "max", and "min". The first two subscripts relate to sloping ground tests and denote the value in the direction of the initial static shear stress (or slope) and perpendicular to the initial stress, respectively (see Fig. 2). If no slope exists the terms "X" and "Y" are used to differentiate the two horizontal directions.

If common terms (e.g. shear strain (γ) or shear stress (τ)) are used without subscripts, the magnitude of the parameter—regardless of direction—is intended. It is important to note that it is the magnitude of normalized shear stress and shear strains that are presented in many of the figures provided in this paper. This is done because (1) the choice of "principal" direction is often arbitrary and (2) the data plots provided are far more meaningful when the magnitude is used. This point is stressed because the plots are similar to those the reader is perhaps used to and this can potentially lead to misunderstanding.

Among the common definitions used in this paper are the r_u, α, and CSR. The term r_u is the normalized pore pressure and is defined as u/σ'_c where u is the pore pressure and σ'_c is the initial vertical effective stress to which the sample was consolidated. An initial static shear stress is applied to replicate either the presence of a structure or sloping ground conditions during testing. The resulting α-value is the normalized initial static shear stress (τ_c/σ'_c). CSR has commonly been defined in uni-directional testing as $\Delta\tau/2$. In multi-directional testing the change in shear stress is defined along a single line and is, therefore, a vector distance and not a change in the absolute value. Examples are shown in Fig. 2.

One new term, shear stress ratio (SSR), has been used extensively in this report to note the normalized shear stress magnitude (τ/σ'_c) at a particular point in time during loading. This should not be confused with CSR. While the SSR is defined at each time-step during loading (and is continually changing), a single CSR is defined

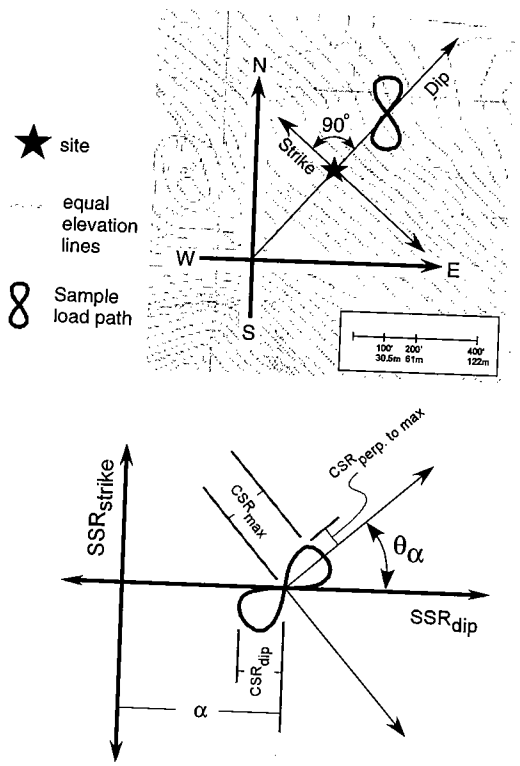

Fig 2: Bi-Directional Parameter Definitions

Table 1: SUMMARY OF BI-DIRECTIONAL TESTING PERFORMED

- Data shown below for each test: Test Name, Relative Density (D_r), Cyclic Stress Ratio in maximum direction (CSR_{max}), Normalized Initial Static Shear Stress (α), Data quality class
- Each test is first noted with the relevant test information in the most appropriate category. Tests that are useful for assessing additional categories also are noted in italics in the appropriate category.
- Extensive one-directional testing on Monterey #0/30 sand using the UCB Bi-directional device was performed as a companion project. For test data refer to Wu et al. (2003)

Plan View Test Path *(dashed line=α)*	**Medium Density (D_r<70%)**		**Dense (D_r>70%)**	
	Low CSR (<0.3)	**High CSR (>0.3)**	**Low CSR (<0.3)**	**High CSR (>0.3)**
1-Directional Linear Paths				
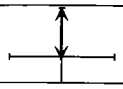				Ms66cyck, 78, 0.51, 0.29, A Ms67cyck, 83 0.48, 0.15, A
2-Directional Linear Paths				
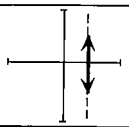	Ms20cyck, 64, 0.24, 0.08, A Ms61cyck, 63, 0.26, 0.13, A	Ms50cyck, 59, 0.43, 0.24, A Ms55cyck, 65, 0.62, 0.35, A Ms56cyck, 70, 0.46, 0.40, A		Ms73cyck, 89, 0.44, 0.12, A
Figure-8 Paths				
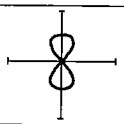	Ms33cyck, 56, 0.25, 0.02, A Ms40cyck, 68, 0.24, 0.02, A Ms41cyck, 63, 0.23, 0.01, A	Ms42cyck, 62, 0.39, 0.03, A		Ms54cyck, 76, 0.45, 0.03, B *Movement in horizontal LVDT during sample preparation*
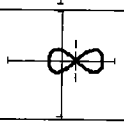	Ms38cyck, 63, 0.23, 0.08, A	Ms51cyck, 63, 0.44, 0.22, A Ms52cyck, 65, 0.50, 0.46, A *Ms48cyck*		Ms72cyck, 86, 0.44 0.23, A
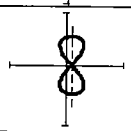	*Ms33cyck*	Ms37cyck, 61, 0.36, 0.18, A *Ms42cyck*	Ms19cyck, 78, 0.23, 0.12, A Ms26cyck, 80, 0.19, 0.20, A	Ms65cyck, 83, 0.47, 0.07, A
Oval/Circular Paths				
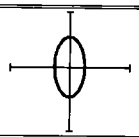	Ms23cyck, 68, 0.21, 0.02, A Ms30cyck, 68, 0.23, 0, A Ms31cyck, 65, 0.25, 0, A Ms43cyck, 48, 0.12, 0, A	Ms44cyck, 68, 0.40, 0.02, A Ms34cyck, 70, 0.35, 0.02, A	Ms58cyck, 80, 0.27, 0.05, ,B *Large drop in one vertical LVDT*	Ms68cyck, 82, 0.44, 0.05, A
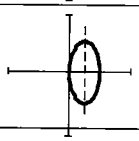	*Ms23cyck* *Ms35 cyck*	Ms49cyck, 61, 0.45, 0.24, A Ms59cyck, 55, 0.38, 0.19, A *Ms34cyck*	Ms25cyck, 75, 0.22, 0.23, A	Ms60cyck, 73, 0.46, 0.21, A Ms69cyck, 87, 0.48, 0.24, A Ms71cyck, 86, 0.47, 0.14, A
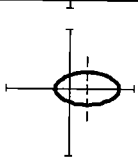	Ms35cyck, 67, 0.23, 0.08, A Ms36cyck, 69, 0.22, 0.12, A Ms45cyck, 58, 0.25, 0.27, A Ms46cyck, 68, 0.23, 0.11, A Ms57cyck, 60, 0.25, 0.16, A *Ms27cyck*	*Ms47cyck*	Ms63cyck, 79, 0.26, 0.13, A	Ms53cyck, 72, 0.42, 0.42, A Ms70cyck, 85, 0.46, 0.42, A
Miscellaneous Paths (all medium density, low CSR)				
MISC	Half-circle Ms32cyck, Dr =62%, B	Cropped oval Ms27cyck, Dr =66%, A Ms47cyck, Dr =58%, A		Cropped figure-8 Ms48cyck, Dr =62%, A

along each line in space for a given test. Another new term is the normalized effective vertical stress. This is defined as (σ'_v/σ'_c). This parameter is useful because (1) it allows for direct comparison of vertical effective stress and r_u at any point in a test ($\sigma'_v/\sigma'_c \approx 1-r_u$) and (2) tests with different initial vertical effective stresses can be directly compared.

RESULTS

Overview

When considering the differences in pore pressure behavior between uni-directional and multi-directional loading, it is useful to recognize that there are two distinct phases of pore pressure behavior in each test. The first is the period of excess pore pressure generation, which occurs from the start of the test to the point where the failure envelope is met. During this period, the maximum pore pressure for each cycle increases until an asymptotic value is reached—at which time it becomes relatively constant during subsequent cycles.

The maximum asymptotic value of the normalized pore pressure is the limiting pore pressure ($r_{u,lim}$). For example, the tests in Fig. 3 (C, E, and F) show a movement towards higher pore pressures (lower effective stresses) until a limiting pore pressure is reached, at which point the stress path plots (E and F) of each cycle overlap and r_u reaches its asymptotic value. Because r_u at each point is equivalent to $1-(\sigma'_v/\sigma'_c)$, the x-axes of the three plots are equivalent.

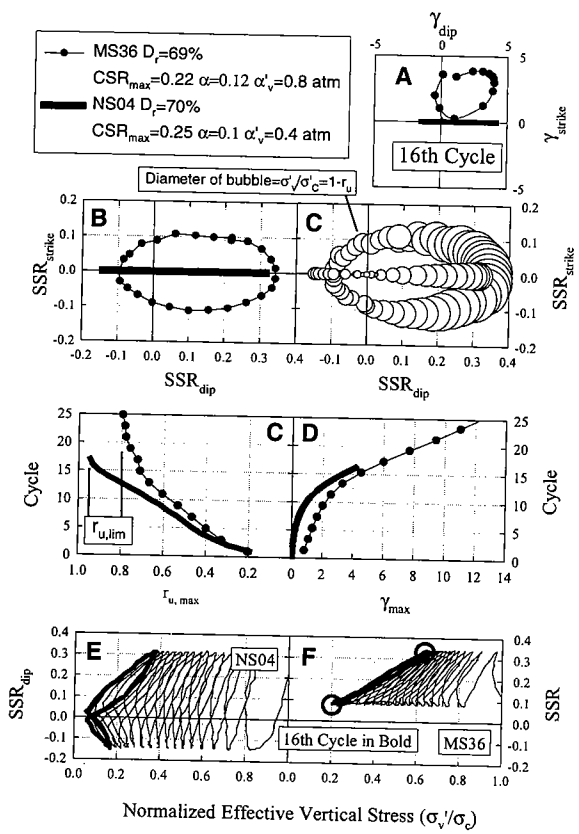

Fig 3: Comparison between linear and oval tests

Multi-directional Loading and Pore Pressure Generation

Results from this study indicate that $r_{u,lim}$ values are typically reached more rapidly under multi-directional loading than in "equivalent" uni-directional tests (i.e. tests with the same D_r and CSR_{max}). The rotation of stresses in the horizontal plane—which occurs only in multi-directional loading—likely plays a large role in the increased rate of pore pressure development by aiding particle rearrangement and densification of the material.

This result is consistent with results from the limited bi-directional testing that is available. Only two previous simple shear studies have been performed using regular bi-directional load paths similar to those presented in this paper [4,5,6] The load path applied in the previous series are shown in Fig. 1. Results from the oval and figure-8 level-ground tests presented here are compared with results from the testing program previously conducted by [4], which included oval and circular stress paths imposed on Toyoura sand samples.

Results from [4] are presented in the upper plot in Fig. 4, which shows the number of cycles to failure (as defined as 3% single amplitude strain) for level ground tests with a variety of aperture ratios (AR). The aperture ratio is defined on Fig. 4. An AR of 0 is a uni-directional test, an AR of 1 denotes a circular test, and intermediate values denote ovals.

The lower plot in Fig 4 presents results from the testing series introduced here. The curve for AR=0 is estimated from the triggering curves for Monterey #0/30 sand presented by [3]. Also shown are results from individual oval and figure-8 tests (AR=0.5) and circular tests (AR=1).

The results from these studies show similar trends in behavior for typical CSR_{max} values, even though the sands, relative densities, and initial confining stresses used in the two studies differ significantly. These trends include a general decrease in liquefaction resistance with both an increased aperture ratio (AR) and increased cyclic stress ratio, CSR_{max}. Both studies also show a similar reduction in additional effect as the aperture ratio increases.

While the behavior of the samples tested under typical CSR values are consistent, the behavior of tests 42, 44, and 68 is somewhat unexpected. Unlike in [4], this research found that in some cases the application of a second direction of loading was detrimental. These are tests with very high CSR_{max} values that are expected to fail within a cycle or two. The reason for this seemingly counter-intuitive behavior is discussed in following sections.

The Effect of Stress Reversal and Initial Static Shear Stress on Pore Pressure Generation

Liquefaction cannot occur unless individual soil grains can move relative to each other and densify. This densification occurs as a result of the rapid application of shear stresses on the soil. Many sand layers further require that the loading be cyclic for the material to sufficiently densify. For this reason, shear stress reversal has long been know to play an important role in liquefaction.

The influence of stress reversal is relatively straightforward in one-directional testing. However, even the basic definition of "stress reversal" must be reassessed when considering multi-directional loads. Because no rotation of stresses occurs in the horizontal plane in one-directional testing, the term "stress reversal" implies that stresses are completely removed and then applied in the opposite direction at least twice in every cycle. Additionally, the incremental stress always lies within a single unchanging line.

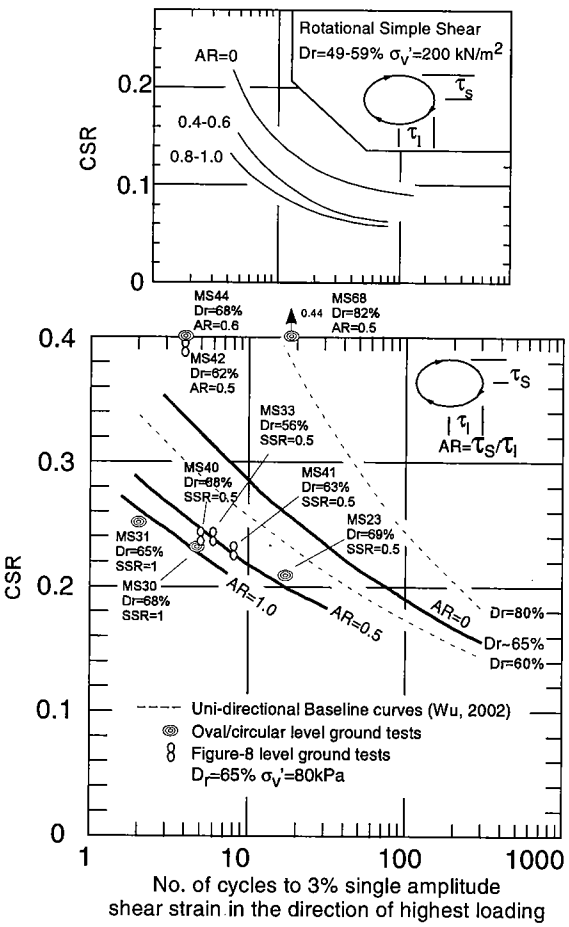

Fig. 4: Comparison of results from (above) Ishihara and Yamazaki (1980) and this study (below) for level-ground tests

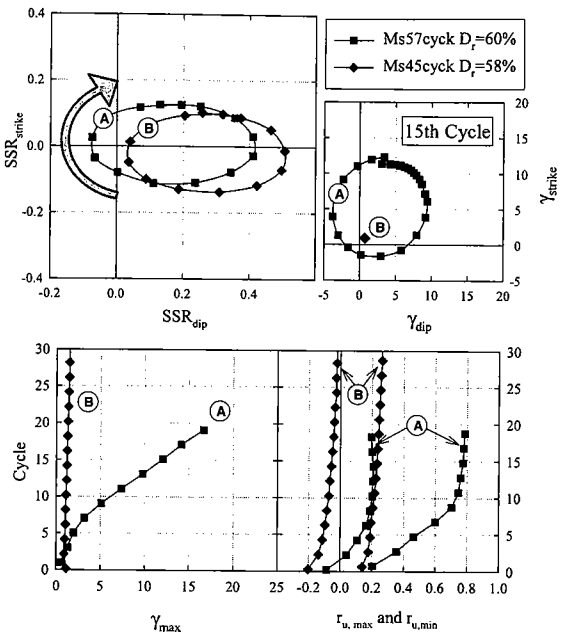

Fig. 5: Comparison of oval dip-oriented tests with increasing α-values

By contrast, in multi-directional loading the shear stresses can rotate to any direction (i.e. rotate 180 degrees). In addition, they can do so without going through a point of zero shear stress. This is the case for the oval test in Fig. 3. Clearly, in multi-directional testing stress reversal can imply either (1) stress removal/release (as in a uni-directional test), (2) rotation of the stress on the horizontal plane, or (3) some combination of both. In multi-directional loading the terms "stress release", "stress release and reversal", and "stress rotation" may be more appropriate. In actual seismic loading, the reversal is almost exclusively some combination of stress release and rotation.

In uni-directional testing, a sufficiently large initial static shear stress ratio (i.e. high α) can decrease the potential for excess pore pressure generation by keeping the grains locked together. This occurs where α exceeds CSR_{dip}, as shown in Fig. 5 (Test 45cyck) for a bi-directional test. Interestingly, the full unlocking of soil grains in uni-directional loading requires not only the removal of shear stresses, but also some loading in the uphill direction, as can be seen in Fig. 3(E). Uni-directional simple shear tests with very small amounts of stress reversal have shown the same limited behavior as tests with no stress reversal [5,7,8].

Very high α-values can also prevent liquefaction in multi-directional tests, though the α-values required may be much higher than the equivalent uni-directional tests, depending on the stress path. However, in contrast to uni-directional loading, there are also stress paths for which, a very small amount of reversal can produce large pore

pressures. This results in an abrupt change (and some volatility) in behavior with a slight change in α.

The effect of stress reversal can be seen in Fig 5, which compares two tests, with similar CSR_{max} and relative density values, but with differing α-values. Here the differences in both pore pressure generation (shown as maximum and minimum values for each cycle) and strain behavior are striking. The small push in the uphill direction in test (A) allows the principal horizontal stresses to rotate a full 360 degrees. By contrast, the higher α-value in test (B) resulted in no stress reversal in the dip direction, and only limited stress rotation of approximately 90 degrees. This can be further contrasted with uni-directional testing in which 180 and 0 degrees of reversal would occur for these CSR_{max} and α-values, respectively.

Fig 6 shows the importance of stress rotation in multi-directional tests by comparing tests with similar CSR_{max} values and stress reversal levels in the dip direction, but with different orientations. There are two tests with different densities shown for each orientation. The orientation of the tests leads to a situation where one set has a much higher degree of rotation, while the other has a much higher maximum shear stress.

The results were consistent between both sets of tests, with the strike-oriented tests showing both larger cyclic and permanent strains. This indicates that that the amount of shear stress reversal/rotation is more important than the maximum shear stress imposed. One may also note that the shear strains of the strike-oriented tests show permanent movement in both the strike and dip directions. This occurs because at each point when the highest pore pressure (and highest degree of softening) is reached, the load path is moving in the same direction.

The Relationship between Shear Stress and Post-Triggering Pore Pressure Behavior

Once the limiting pore pressure ($r_{u,lim}$) has been achieved in a given test, the pore pressures measured throughout each cycle of uniform loading show repetition in behavior. Fig 7 shows the limiting maximum and minimum pore pressures that occur in each liquefied test in the series plotted against the shear stress ratios at which each of the values occur. As an example, the values plotted for tests MS36cyck are highlighted by the circles on Fig 3(F). When this $r_{u,lim}$ and $r_{u,lim,min}$ data is plotted, it shows a roughly inverse-linear relationship with shear stress. The few values that plot noticeably below the trend lines are cases where there is no shear stress reversal in the dip direction, but where the sample still liquefied due to large shear stresses in the strike direction (e.g. Tests MS60cyck and MS69cyck in Fig. 5).

These results are very similar to those obtained in an earlier program for an equivalent parameter by [5]. This testing on Sacramento River Sand used a linear stress path that included an initial static driving shear stress (i.e. $\alpha>0$) and was oriented in the strike direction, as shown in Fig 1.

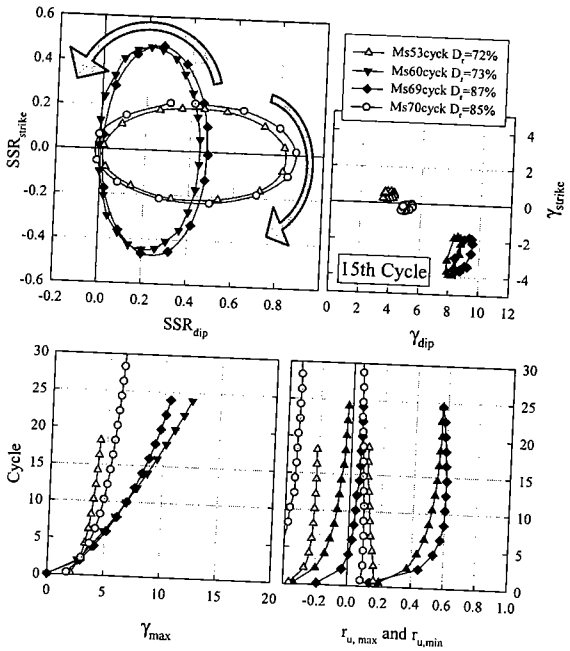

Fig 6: Comparison of oval strike and dip-oriented tests with no reversal in dip direction

The lines that are shown on Fig 7, bound the plots of $r_{u,lim}$ versus α for the tests performed by [5]. Because α was equivalent to SSR_{min} in the stress path used in this series, a direct comparison can be made.

This inverse relationship between shear stress and post-triggering pore pressure can be explained by dilation of the soil particles. In both uni- and bi-directional tests, dilation causes a drop in pore pressure as limiting strains are reached and particles are forced to move over each other. In the case of uni-directional loading, this relative motion must occur within a single plane. In multi-directional loading there is more freedom of movement,

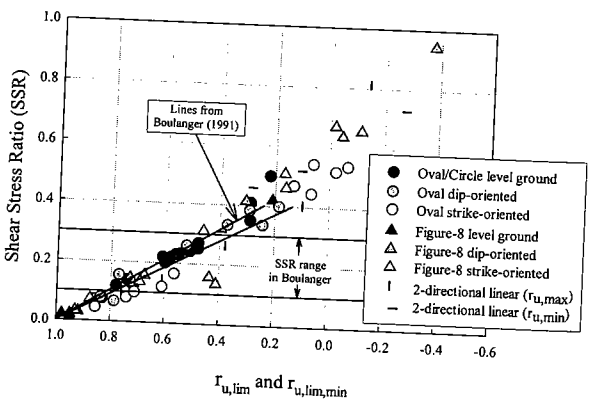

Fig 7: comparison of normalized pore pressure values achieved during a "liquefied" cycle as a function of the shear stress ratio

making the resulting dilation less problematic but still evident.

There are also cases, however, when the drop in pore pressure due to shear stress is large enough that the soil cannot soften or softens more slowly than expected. This occurs with certain load paths in which the shear stresses imposed remain very large. This is the case with Tests MS42cyck, MS44cyck and MS68cyck in Fig. 4.

The inverse relationship between SSR and r_u values is foreseeable because the r_u values plotted are principally located on the failure envelope that exists for each test. For example, in Fig. 3 (F) every point of the final cycle remains on the failure envelope. It is only during unloading in some tests that the stress state leaves the failure plane (see Fig. 3 (E)). The section below examines this behavior in more detail.

Shear Stress Rotation and Pore Pressure Lag

As shown in Fig 3(E) there is a lag in pore pressure during the unloading phase of a uni-directional test. While some multi-directional tests exhibit this behavior, many others do not. The data indicates that the lag in pore pressure that occurs during the unloading phase in some types of test is eliminated if rotation of the shear stresses in the horizontal plane occurs as the shear stress is reduced. For example, stress path categories in which a high degree of rotation is constantly occurring (e.g. the oval test in Fig. 3) show no pore pressure lag at all.

Many figure-8 tests represent a mix of the two conditions with both a high degree of rotation and a high degree of release occurring in different part of the stress path. Fig 8 presents a single cycle of two different figure-8 tests that have each been separated into four regions. In two of the regions shown in the top figure (A and C) shear stresses are being removed and again reapplied with little stress rotation. In regions (B) and (D) loads change, while a higher degree of rotation is occurring. It can be seen that a pore pressure lag occurs in this test, but only where little shear stress rotation in the horizontal plane occurs during unloading (part C). Once the rotation again increases (at D) the sample quickly returns to the failure envelope. Similarly, in the lower plots there are two regions ((A) and (C)) where the unloading is occurring without any rotation and a large pore pressure lag can be seen. This lag does not occur in (B) and (D) due to rotation.

The overall behavior can be explained if we consider the particle behavior. If there is no rotation of the horizontal stresses during release, the particles would be forced to move in a plane (as in uni-directional tests). This may allow them to become locked together and resist movement as the stress is released, which in turn prohibits pore pressure generation. The grains remain locked until sufficient stress has been released. By contrast, if a stress is applied laterally to the sample as the load is being released, it is difficult for the grains to remain locked together. When locking is prohibited, pore pressures will be developed as expected.

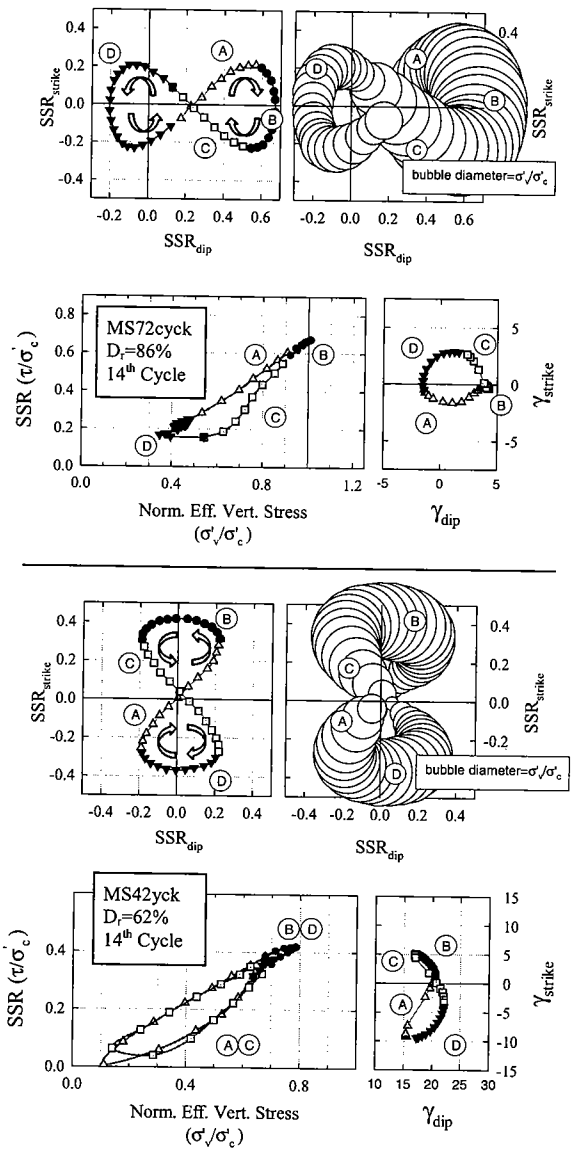

Fig 8: Plan view stresses and strains, normalized vertical effective stresses, and stress path for two figure-8 test

Pore Pressure and Liquefaction Triggering

There are several examples presented in this paper of tests that developed large strains while exhibiting $r_{u,lim}$ values far less than 1.0. These include Test MS36cyck (Fig 3), MS57cyck (Fig. 5), Tests MS60cyck and MS69cyck (Fig. 6), and Test MS72cyck (Fig 8), which developed $r_{u,lim}$ values of 0.8, 0.8, 0.6 0.6, and 0.7, respectively. These stress paths maintain a relatively large shear stress throughout testing, and thus cannot produce large pore pressures due to the inverse relationship between shear stress and pore pressure discussed above. In addition, all the data shown in Fig. 7 is from tests that achieved 6% double amplitude strains. These strains

occurred even though the $r_{u,lim}$ value achieved in many of the tests was well below 1.0.

The idea of r_u =1.0 as a definition of liquefaction results from the preponderance of uni-directional testing. Because there is complete removal of shear strains twice in each test, $r_{u,lim}$ values of approximately 1.0 occur. In contrast, results from this testing program seem to imply that once an r_u value of approximately 0.65 or higher is reached that sufficient softening occurs to start a positive feedback system. The softening allows increased strains, which in turn allows for more efficient densification and increasingly larger strains in each cycle. For example, the strains in Fig 3(D) accelerate at r_u values well below 1.0.

Further consider the tests shown in Fig 3. The minimum SSR values imposed on the oval test is approximately 0.1, by contrast the minimum SSR in the uni-directional test is 0. The results are clearly evident in Fig. 3(C) as it is only at the point of zero shear stress in the uni-directional tests that the effective stress approaches zero.

SUMMARY

While the behavior of liquefiable soils under multi-directional loading is far too complex to fully address here, the general behaviors discussed in this paper can be summarized.

- The addition of shear stress in a second horizontal direction tends to result in quicker attainment of $r_{u,lim}$. The biggest change in liquefaction resistance occurs when the load is first applied in the second direction. A further increase in the load in the second direction continues to lower resistance, with declining effect.
- As with uni-directional loading, increasing the magnitude of the shear stresses tends to reduce the number of cycles to the limiting pore pressure. However, it can also reduce the limiting pore pressure to the point where significant softening is not induced in the sample in certain load paths.
- After the limiting pore pressure has been achieved in a given test, the pore pressures measured at any point during a cycle exhibits a (roughly) inverse linear relationship with the shear stress at that point. This relationship can be estimated from the failure envelope, though some exceptions do apply.
- The assumption that the excess pore pressure within a sample must approach the total vertical stress (resulting in $r_u \approx 1.0$) in order for "liquefaction" to be achieve must be reassessed based on results showing that a large number of tests exhibited large strains with relatively low maximum pore pressures ($r_{u,max}$=0.7or less). This logically follows once it is recognized that (a) there is a relationship between minimum shear stress and maximum excess pore pressure and (b) few multi-directional tests experience points of zero shear stress.
- As with uni-directional loading, a sufficiently large initial static shear stress ratio (i.e. high α) can increase resistance to liquefaction triggering by greatly reducing the degree of stress reversal and, thus, the potential for excess pore pressure generation. However, a small amount of reversal can produce large pore pressures in some multi-directional load paths incorporating rotation. This results in an abrupt change (and some volatility) in behavior. In addition, large strains do occur with no reversal (in the classic sense) occurring for some stress paths.
- The lag in pore pressure generation that occurs during the unloading phase of each cycle in uni-directional testing is reduced or eliminated if rotation of the shear stresses in the horizontal plane occurs during the shear stress release.

ACKNOWLEDGMENTS

Financial support for this research was provided by the NSF, CAREER award CMS-9623979, by the Pacific Earthquake Engineering Research Center, through project 2051999, by a National Science Foundation Graduate Research Fellowship and an EERI/FEMA NEHRP Graduate Research Fellowship. On-going support for publication and presentation provided by Ove Arup and Partners California, Ltd (Arup)

REFERENCES

[1] Boulanger, R. W., Chan, C. K., Seed, H. B., and Seed, R. B. (1993). "A low-compliance bi-directional cyclic simple shear apparatus." Geotech. Testing J., 16(1), 36-45.

[2] Kammerer, A., Pestana, and Seed, R. (2002) "Undrained Response of Monterey 0/30 Sand Under Multidirectional Cyclic Simple Shear Loading Conditions", Geotechnical Engineering Research Report No. UCB/GT/02-01, University of California, Berkeley, July 2002.

[3] Wu, J., Seed, R.B., and Pestana, J.M. (2003) Liquefaction triggering and post-liquefaction deformation of Monterey 0/30 sand under uni-directional cyclic simple shear loading", Univeristy of California, Berkeley Geotechnical Engineering Report No. UCB/GE-2003/01, April 2003

[4] Ishihara, K. and Yamazaki, F. (1980). "Cyclic simple shear tests on saturated sand in multi-directional loading." Soils and Foundations, 20(1), 45-59.Harder, L. F. and Boulanger, R. W. (1997). "Application of K_σ and $K\alpha$ Correction Factors." Rep. No. NCEER-97-0022, NCEER, Buffalo, NY.

[5] Boulanger, R. W. and Seed, R. B. (1995). "Liquefaction of sand under bi-directional monotonic and cyclic loading." J. Geotech. Engng., ASCE, 121(12), 870-878.

[6] Boulanger, R. W., Seed, R. B., Chan, C. K., Seed, H. B., and Sousa, J. B. (1991b). "Liquefaction behavior of saturated sands under uni-directional and bi-directional monotonic and cyclic simple shear loading." Rep. No. UCB/GT-91/08, University of California, Berkeley.

[7] Harder, L. F. and Boulanger, R. W. (1997). "Application of $K\sigma$ and $K\alpha$Correction Factors." Rep. No. NCEER-97-0022, NCEER, Buffalo.

[8] Vaid, Y. P. and Finn, W. D. L. (1979). "Static shear and liquefaction potential." J. Geotech. Eng. Div., ASCE, 105 (GT10), p.123